clear that provided problems of specimen mounting can be overcome, the Bragg angles of any two crystals can be compared to about 0·1 % of the width of the pseudo non-dispersive double-crystal rocking curve. Since at exact equality the rocking curves are symmetric, there is no limit in principle other than that set by counting statistics on the precision with which lattice parameters can be compared.

Finally we should point out that it is not a 'lucky chance' which makes these measurements possible. By using sufficiently high orders of Bragg reflexions it is inevitable that lattice-parameter matches occur in different materials at some accessible temperature.

References

BAKER, T. W., GEORGE, J. D., BELLAMY, B. A. & CAUSER, R. (1966). *Nature, Lond.* **210**, 720–721.
BOND, W. L. (1960). *Acta Cryst.* **13**, 814–818.
BOND, W. L. (1961). *J. Sci. Instrum.* **38**, 63–64.
DESLATTES, R. D. & HENINS, A. (1973). *Phys. Rev. Lett.* **31**, 972–974.
GIBBONS, D. F. (1958). *Phys. Rev.* **112**, 136–140.
HART, M. (1969). *Proc. Roy. Soc.* A**309**, 289–296.
LARSON, B. C. (1974). *J. Appl. Phys.* **45**, 514–518.
THOMSEN, J. S. & YAP, F. Y. (1968). *Acta Cryst.* A**24**, 702–703.

On the Application of Phase Relationships to Complex Structures. VIII. An Extension of the Magic-Integer Approach

By J. P. DECLERCQ AND G. GERMAIN

Laboratoire de Chimie Physique et de Cristallographie, Université de Louvain, Louvain-la-Neuve, Belgium

AND M. M. WOOLFSON

Department of Physics, University of York, England

A magic-integer approach, called the *P–S* set method is described. A primary (*P*) set of reflexions contains some which fix the origin and enantiomorph and others expressed symbolically in magic-integer form. Probable phases for a secondary (*S*) set of reflexions are derived, also in symbolic form, from single triple-phase relationships containing a pair of *P* reflexions. Relationships which link the combined *P* and *S* sets give rise to the terms of a Fourier map, the peaks of which indicate likely sets of phases for all the reflexions under consideration. These sets of phases are used as starting points for the computer program *MULTAN*. The process is completely automated and is illustrated by the solution of the structure of cephalotaxine, $C_{18}H_{21}O_4N$, the space group of which is *C*2 with two molecules in the asymmetric unit.

Introduction

In a recent paper White & Woolfson (1975) described a technique whereby phases may be represented to a sufficient degree of approximation in a symbolic form such that a single symbol may be used to represent several phases. Thus for a suitable set of *m* integers – $n_1, n_2, \ldots, n_m$ – one may write

$$\varphi_r = n_r x \bmod (1), \quad r = 1 \text{ to } m, \tag{1}$$

where the phase angles, φ, are expressed in cycles and the set of equations is approximately satisfied for some value of *x* in the range $0 \le x < 1$.

Trials by White & Woolfson (1975) showed that a simple application of magic integers, in a way which is a blend of the symbolic-addition and multiple-solution

approaches, could lead to complete and straightforward solutions of structures which had been solved rather tortuously from *E* maps given by the *MULTAN* computer package. The extension of the magic-integer approach which is described in this paper is even more powerful and has solved a number of known test structures for which the automatic *MULTAN* procedure had failed completely.

The *P-S* sets method

In explaining the new magic-integer approach we shall use as an example the structure of cephalotaxine, $C_{18}H_{21}O_4N$, the form of the molecule of which is shown in Fig. 1. The space group is *C*2 with $a = 22.84$, $b = 8.15$, $c = 19.54$ Å and $\beta = 117.7°$. There are two mole-

cules in the asymmetric unit, so that there are 46 non-hydrogen atoms to be found. Many attempts to solve the structure with *MULTAN* failed miserably and the structure was finally solved by a Patterson vector-search approach with a model taken from the solution of the structure of the bromo derivative.

When phases, with magic-integer representation, are linked together in the form of triple-product phase relationships then there are four influences which cause the value of the invariant, so expressed, to deviate from 0 mod (1). These influences are the errors in representing the three phases and the actual value of the invariant itself. Errors in representing phases are inherent in the magic-integer approach; they are the price which has to be paid for the advantage of being able simultaneously to handle a large number of unknown phases. However we can attempt to reduce the fourth influence as far as possible and this we do by initially restricting our attention to only the very strongest available relationships. In the case of cephalotaxine the routine *NORMAL*, the first part of *MULTAN*, was run to convert the raw data into E's, the normalized structure factors, and a subset of 350 strongest E's was selected. The *MULTAN* routines

SIGMA 2 and *CONVERGENCE* were then used to find the strongest 100 triple-phase relationships (tpr's) and it was checked that they contained reflexions in terms of which the origin and enantiomorph could be fixed. It requires two reflexions to fix the origin in this space group; one special reflexion with indices $h0l$ and with l odd, if allocated the phase 0 (or π), will select the origin on one of the two distinct twofold axes. Allocation of a definite phase to a reflexion of type $h1l$ will then uniquely fix the origin on that twofold axis. The enantiomorph can now be selected by choosing a general reflexion of type hkl and restricting its phase either to the range $0-\pi$ or to the range $\pi-2\pi$. In accordance with the general *MULTAN* philosophy this can be done by restricting possible phases to one or other of the pairs of values $(\pi/4, 3\pi/4)$ or $(-\pi/4, -3\pi/4)$.

For cephalotaxine the selection made is shown in Table 1. The origin-fixing reflexions are given the values found from the known structure – there is no loss of generality in this procedure – and the enantiomorph-fixing reflexion is restricted to the pair $(-\pi/4, -3\pi/4)$, the value from the solved structure being 236°. In what follows this phase is assumed to be

Table 1. *Selection of reflexions for cephalotaxine*

Code	h	P k	l	Phase or symbol	Code	h	S k	l	tpr	Phase or symbol
5	18	0	$\bar{9}$	180°						
36	25	1	$\overline{12}$	327°						
6	0	2	15	225°						
					50	18	2	6	$\varphi_{50}+\varphi_5-\varphi_6$	45°
					48	7	1	$\bar{3}$	$\varphi_{48}-\varphi_5-\varphi_{36}$	147°
9	3	5	8	$5y$						
					54	3	3	$\bar{7}$	$\varphi_{54}+\varphi_6-\varphi_9$	$5y+135°$
24	17	5	3	$7y$						
					82	1	5	$\overline{12}$	$\varphi_{82}-\varphi_5-\varphi_{24}$	$7y+180°$
					62	14	0	$\bar{5}$	$\varphi_{62}+\varphi_9-\varphi_{24}$	$2y$
15	23	3	$\overline{14}$	$7x$						
29	13	1	$\bar{5}$	$9x$						
32*	13	1	$\overline{20}$	$9y$						
					64	10	4	6	$\varphi_{64}-\varphi_{15}-\varphi_{32}$	$7x+9y$
					96	16	6	3	$\varphi_{96}-\varphi_9-\varphi_{29}$	$9x+5y$
33	3	3	11	$11x$						
61*	15	3	$\overline{20}$	$5z$						
58	0	4	3							
					2	8	0	6	$\varphi_2+\varphi_{15}-\varphi_{61}$	$-7x+5z$
					20	0	6	12	$\varphi_{20}-\varphi_{58}-\varphi_6$	
19	14	4	$\bar{4}$							
					245	14	2	$\overline{19}$	$\varphi_{245}+\varphi_6-\varphi_{19}$	
21	11	5	7	$7z$						
49*	14	4	$\overline{19}$	$11x$						
					279	7	5	$\overline{16}$	$\varphi_{279}-\varphi_5-\varphi_{21}$	$7z+180°$
					74	6	0	$\bar{4}$	$\varphi_{74}+\varphi_{21}-\varphi_{24}$	$7y-7z$
22	18	2	$\overline{21}$	$5x$						
					11	18	0	$\bar{6}$	$\varphi_{11}+\varphi_{22}-\varphi_6$	$-5x+225°$
					65	5	5	7	$\varphi_{65}-\varphi_{15}-\varphi_{22}$	$12x$
					104	4	4	10	$\varphi_{104}-\varphi_5-\varphi_{49}$	$11x+180°$
					110	21	3	$\overline{13}$	$\varphi_{110}-\varphi_9+\varphi_{22}$	$-5x+5y$
136	17	3	$\bar{2}$							
					1	6	0	$\overline{12}$	$\varphi_1+\varphi_{15}-\varphi_{136}$	
					3	14	0	$\overline{13}$	$\varphi_3-\varphi_{33}+\varphi_{136}$	
7	8	4	$\overline{18}$	$9z$						
					219	8	6	$\bar{3}$	$\varphi_{219}-\varphi_6-\varphi_7$	$9z+225°$
30	7	3	$\overline{18}$	$11z$						
					16	24	2	$\overline{15}$	$\varphi_{16}-\varphi_{24}+\varphi_{30}$	$7y-11z$

$-3\pi/4$ but in practice both values would be considered in turn.

These three reflexions are placed in what we call the *primary* (P) set and they are shown as the top three of the P set in Table 1 with their angles given in degrees. A process is now begun with the following objective – to add a predetermined number of reflexions to the P set which, together with the three reflexions already in the P set, will give rise to the greatest number of determinations of probable phase for other reflexions from single tpr's contained in the strongest 100 tpr's. The dependent reflexions, whose probable phases are given in terms of the phases of pairs of P set reflexions, are termed the *secondary* or S set and these are also shown in Table 1.

The algorithm by which this process is carried out will be explained for cephalotaxine where the number of P reflexions to be added to the origin and enantiomorph-fixing reflexions is 15. First the three top reflexions in the P set are examined to see if they alone give any S set reflexions. It is found that the phases of reflexions with code numbers 48 and 50 can be determined by single tpr's from the top three reflexions in the P set and these two are assigned to the S set. The procedure now followed is to find from the 100 tpr's that reflexion which, when added to the existing P set members, will give the maximum number of S reflexions. Thus reflexion 9, when added to the P set, gives reflexion 54 in the S set. Then follows reflexion 24 in the P set giving two contributions to the S set, reflexions 82 and 62. It is then found that no reflexion could be selected so as to give S set contributors and in this case the reflexion which occurs most frequently in the 100 tpr's is added to the P set; this is reflexion 15.

At this stage it is found that reflexion 29, if added to the P set would give two members of the S set, those with codes 32 and 96, but it is also found that reflexion 32 as a member of the P set would also give an S set contributor. It has been found by experience that the best thing to do in such a situation is to assign reflexion 32 to the P set. It is marked with an asterisk in Table 1 and two other P set reflexions which have arisen in the same way are similarly marked. A continuation of the procedure as outlined above eventually gives the complete Table 1.
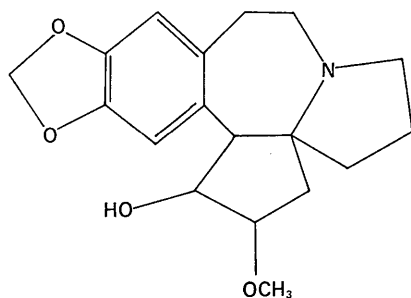

Fig. 1. The form of the molecule of cephalotaxine.

The selection of 15 unknown phases in the primary set was made on the basis of a decision to use the magic-integer sequence (5, 7, 9, 11, 13) with the variables x, y and z. However, before commenting on the allocation of the magic-integer-based symbols we should examine the next stage in the phase-determining process. In this we find all the tpr's which link together the phases in the combined P and S sets other than those tpr's which have been used to obtain S reflexions from P reflexions. There are thirteen of these and they are listed in Table 2. An example will show why it is unwise to allocate magic-integer-based phases in an arbitrary way. We express phase relationship (3), in Table 2, in terms of the phases of primary reflexions only, that is with the phases of secondary reflexions given by the tpr column in Table 1. Then

$$\varphi_{110} + \varphi_{11} - \varphi_{54} \simeq 0$$

implies that

$$(\varphi_9 - \varphi_{22}) + (\varphi_6 - \varphi_{22}) - (\varphi_9 - \varphi_6) \simeq 0$$

or

$$2\varphi_{22} - 2\varphi_6 \simeq 0.$$

Table 2. *Phase relationships for cephalotaxine other than those giving secondary from primary reflexions*

(1)	$\varphi_{30} - \varphi_{36} - \varphi_{50}$		$11z - 12°$
(2)	$\varphi_{30} - \varphi_{48} - \varphi_6$		$11z - 12°$
(3)	$\varphi_{110} + \varphi_{11} - \varphi_{54}$	$-10x$	$+ 90°$
(4)	$\varphi_{21} - \varphi_{48} - \varphi_{104}$	$-11x$	$+ 7z + 33°$
(5)	$\varphi_{21} - \varphi_{36} - \varphi_{49}$	$-11x$	$- 7z + 33°$
(6)	$\varphi_{279} - \varphi_{48} - \varphi_{49}$	$-11x$	$+ 7z + 33°$
(7)	$\varphi_{74} - \varphi_{82} + \varphi_{279}$		$0°$
(8)	$\varphi_{64} - \varphi_{74} - \varphi_{104}$	$- 4x + 2y +$	$7z + 180°$
(9)	$\varphi_{64} - \varphi_{24} + \varphi_{48}$	$7x + 2y$	$+147°$
(10)	$\varphi_{29} + \varphi_{32} - \varphi_6$	$9x + 9y$	$+135°$
(11)	$\varphi_7 + \varphi_{16} - \varphi_{96}$	$- 9x + 2y -$	$2z$
(12)	$\varphi_2 + \varphi_{96} - \varphi_{219}$	$2x + 5y -$	$4z + 135°$
(13)	$\varphi_{33} - \varphi_{61} + \varphi_5$	$11y -$	$5z + 180°$

If φ_{22} is represented by $13x$ then representation of tpr 3 involves $26x$ and we are generating high coefficients for the variables. As was done previously by White & Woolfson (1975) we are going to compute a Fourier map and the term representing tpr 3 would have indices 26,0,0. The larger the indices are then the finer must be the net at the points of which the Fourier map is calculated and the longer it will take to compute. Thus for maximum efficiency we must so assign magic-integer-based symbols to our 15 primary phases that the indices generated by the tpr's in Table 2 have the least possible maximum values. To this end an algorithm has been designed giving the symbolic allocations shown in Table 1 and its success may be judged by the symbolic representation of the phase relationships as shown in Table 2. It will be noticed that primary reflexions 58, 19 and 136 do not appear, even by implication through secondary reflexions, in the tpr's in Table 2 and they are therefore removed from

the phase-determining process. The magic-integer sequence is therefore truncated to (5, 7, 9, 11).

Each of the relationships appears in the form

$$Hx + Ky + Lz + \beta \simeq 0 \bmod (1) \qquad (2)$$

where, now, the constant angle is expressed in cycles. A Fourier map, similar to the ψ map described by White & Woolfson, is now computed. This is

$$\psi(x,y,z) = \sum_r |E^3|_r \cos\{2\pi(H_r x + K_r y + L_r z + \beta_r)\} \qquad (3)$$

where the summation is over all the tpr's in Table 2 and $|E^3|_r$ is the product of the three normalized structure factors for the reflexions involved in the tpr. In fact, as we can see from Table 2 there is not much point in including tpr 7 which is just a constant added to ψ and there are only nine different sets of indices for the terms included in ψ.

The process now continues much as described by White & Woolfson except that the whole process is highly automated. All the steps described up to the present stage, including the allocation of magic-integer-based phases are quite automatic and require no intervention on the part of the program user except to specify the magic-integer sequence he wishes to use.

The ψ map is computed by the *FFT* routine in *MULTAN* and the map is scanned automatically to find the highest 50 peaks. From the values of (x,y,z) for each of these peaks first trial values are found for each of the phases, for those in both the secondary and the primary sets, by substitution in their magic-integer-based symbolic representations in Table 1. However this can only be done for 12 primary and 16 secondary reflexions excluding reflexions 58, 19 and 136 in the primary set (as previously mentioned) and reflexions 20, 245, 1 and 3 in the secondary set since these did not contribute to the ψ map. The 28 phases so found, plus the origin and enantiomorph fixing reflexions, are given in Table 3 under the column 'First approximation'.

The next stage is to consider *all* the relationships linking the fifteen reflexions in the P set together with the 16 reflexions in the S set. There are 29 of these, the 13 given in Table 2 together with the 16 which were used to derive those secondary reflexions given in Table 3.

We construct the function

$$\zeta(\varphi_6, \varphi_9, \ldots, \varphi_{219}, \varphi_{16}) = \sum_{r=1}^{29} |E^3|_r \cos(S_r) \qquad (4)$$

where the S's on the right-hand side are tpr's expressed in terms of φ's from φ_6 to φ_{16} in Table 3 and which may also contain a constant angle component. The origin-fixing reflexions are not allowed to change but the remainder are changed by the parameter-shift method described by White & Woolfson so as to maximize the value of ζ. In this process each φ is varied independently and the coupling of phases through magic integers is broken at this stage. The results at the end

Table 3. *The derivation of phases from the 'correct' peak of the ψ map for cephalotaxine peak* 39, $x = 0.313$, $y = 0.741$, $z = 0.911$

Code	Symbol	First approximation	Parameter shift	Axis shift	Known phase
5	180°	180	180	180	180
36	327°	327	327	352	327
6	225°	225	211	261	236
9	5y	254	244	9	334
15	7x	69	62	137	189
24	7y	67	84	209	237
29	9x	294	311	326	343
32	9y	241	254	279	215
33	11y	54	19	94	60
61	5z	200	198	273	318
21	7z	136	135	260	256
49	11x	159	171	271	355
22	5x	203	210	260	236
7	9z	72	107	207	126
30	11z	8	357	72	16
50	45°	45	˙31	81	69
48	147°	147	143	168	125
54	5y+135°	29	35	110	139
82	7y+180°	247	262	27	72
62*	2y	174	180	180	180
64	7x+9y	310	305	45	74
96	9x+5y	188	192	342	299
2*	−7x+5z	131	180	180	180
279	7z+180°	316	315	80	77
74*	7y−7z	291	0	0	0
11*	−5x+225°	22	0	0	0
65	12x	272	272	37	95
104	11x+180°	339	353	93	35
110	−5x+5y	51	36	111	158
219	9z+225°	297	320	110	331
16	7y−11z	59	83	133	120

of this process are shown in Table 3 under the heading 'Parameter shift'.

Each of the 50 sets of phases derived after the parameter shift process is used as a starting point for the *FASTAN* section of *MULTAN* resulting in 50 sets of phases for 350 reflexions together with the usual figures of merit. These were then explored in the order suggested by a combined figure of merit by the calculation of E maps followed by the automatic peak-search procedure and line-printer output in graphical form of possible projected molecular fragments (Declercq, Germain, Main & Woolfson, 1973). The third-highest figure of merit corresponded to peak 39 on the ψ map and Table 3 is based on this peak. The phases found from the parameter-shift procedure differed greatly from the known-structure phases but this was due to a shift of origin along the twofold axis. A shift $\Delta y = -0.069$ gave the phases in the penultimate column and with the exception of φ_{219} these compare favourably with the known phases.

The Fourier map derived from peak 39 of the ψ map showed two fragments corresponding to the two molecules in the asymmetric unit, one containing 14 peaks and the other one 19 peaks. Straightforward procedures led from this to a complete solution of the structure.

Other applications of the method

The process described in the previous section is automatic and takes very little computer time, the greatest time being taken by *FASTAN* and the subsequent operations of the *MULTAN* package. It has been successful when applied to a range of structures, all known but all deliberately chosen for the malice they seem to exhibit. The very first structure tried, lithocholic acid, was a spectacular success. With *MULTAN* there had been obtained a fragment of eight atoms, of which three turned out to be spurious, and from this by tangent-formula recycling and Fourier methods one could fight through to the complete structure solution. With the magic-integer approach the final set of phases with the highest combined figure of merit showed every one of the 27 atoms in the molecule.

The least successful application has been to a 69-atom structure ApApA. This could not be solved by a straightforward application of *MULTAN* but could be solved by applying a substantialization technique (Woolfson, 1954) with *MULTAN*. With magic integers the phases from the 17th highest combined figure of merit gave a map with a clear fragment of 19 out of the 69 atoms, from which point tangent-formula recycling and classical Fourier procedures led directly to the solution. In this case the magic-integer approach gave approximately the same result as the substantialization-plus-*MULTAN* method.

Why does the method work?

The feature of the magic-integer approach which makes it so successful is that it enables a large number of phases, and the relationships between them, to be considered simultaneously, which seems to circumvent the problem of the 'weak link' which bedevils many stepwise processes. The penalty which is paid for this advantage is the inaccuracy of representation of phases.

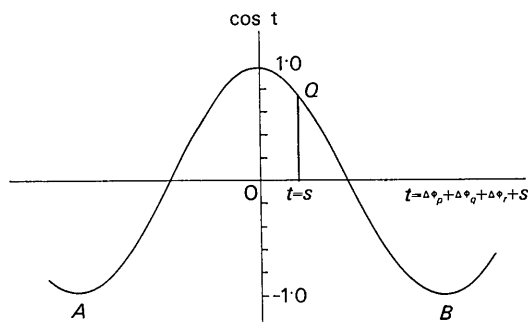The parameter-shift process should, ideally, be able to correct the errors in phases given by the magic-integer representation. The maximizing function contains terms of the general form

$$|E^3| \cos (\varphi_p + \varphi_q + \varphi_r) \qquad (5)$$

where there may be fewer than three unknown φ's if one (or more) of them is a fixed phase. If the errors in the three phases given by the magic-integer representation are $\Delta\varphi_p$, $\Delta\varphi$ and $\Delta\varphi_r$, and the invariant itself has a true value S, then the term will have the initial value

$$|E^3| \cos t$$

where

$$t = \Delta\varphi_p + \Delta\varphi_q + \Delta\varphi_r + S . \qquad (6)$$

The form of the function $\cos t$ is shown in Fig. 2 and in an ideal situation the refinement of phases will cause this cosine to move towards the point Q – that is towards having all the errors in phase equal to zero. However unless the initial value of t is somewhere in the range A to B the refinement procedure will tend to be influenced by this cosine term in a direction which increases, rather than reduces, the errors in the phase. If the value of s deviates significantly from zero then, since the refinement tends to move the value of t towards the peak of the cosine curve, there is once again an in-built error in the system but at least the total error in the three phases introduced by this effect is of order s. If the variance of the triple-phase invariant is V (Karle & Karle, 1966) and that of representing each of the phases by magic integers is ϱ_M^2 then the standard deviation in the distribution of t, regarded as an unknown quantity with a certain probability density, is

$$\varrho_t = (V + 3\varrho_M^2)^{1/2}. \qquad (7)$$

The unknown quantity t will have an approximately normal distribution about zero and hence, if $\varrho_t \simeq \pi/2$, from the statistics of the normal distribution we estimate that only one in 30 or so of the cosine terms should hinder the refinement process.

The situation is different for relationships which involve one or more secondary reflexions. In the most extreme case the value of t would involve the errors in six primary phases and the values of four invariants which, if they all had a standard deviation of $\pi/4$, would give a distribution for t with a standard deviation of $\sqrt{10} \times \pi/4$ or, approximately $3\pi/4$. Thus t would need to stay within $\frac{4}{3}\varrho_t$ of its expectation value for the relationship to be helpful in refinement and this indicates that one in five relationships would hinder refinement.

An analysis along these lines would suggest that individual terms of the type shown in expression (3) should be weighted to take account of the value of ϱ_t and this possibility will be investigated in future work.

Fig. 2. Errors in phase representation keeping the quantity t within the range A to B will tend to be corrected by parameter-shift refinement. Q represents the true value of the triple-phase invariant and is the point towards which 'perfect' refinement would converge.

The limits of application

A question of interest concerns the complexity of structure for which the magic-integer approach might be successful. For a complex structure with one

hundred atoms in the asymmetric unit one may need to use triple-phase invariants with a standard deviation of $\pi/3$ or so. Again, in order to introduce enough magic-integer defined phases, it will be necessary to use long magic-integer sequences with up to eight integers. If a maximum integer of 100 can be tolerated then a root-mean-square error of slightly more than $\pi/4$ will result. If three variables, x, y and z, are used then there will be 24 primary reflexions and, our experience suggests, 70 to 100 secondary reflexions. This will be a large base from which a complete structure solution should be possible. The time requirement for the whole process would be dominated by that to calculate a Fourier map at intervals of $1/400$ in each of three directions. While this is a formidable task it is by no means an impossible one and it would be worth while to put this amount of effort into an operation which offered real hope of success with a major structural problem.

Computational aspects of this project were primarily carried out in the Centre de Calcul, Université de Louvain, and we are grateful for the generous provision of these facilities. We are also grateful to Professor R. B. Bates for providing the data for cephalotaxine and lithocholic acid.

References

DECLERCQ, J. P., GERMAIN, G., MAIN, P. & WOOLFSON, M. M. (1973). *Acta Cryst.* A29, 231–234.
KARLE, J. & KARLE, I. L. (1966). *Acta Cryst.* 21, 849–859.
WHITE, P. S. & WOOLFSON, M. M. (1975). *Acta Cryst.* A31, 53–56.
WOOLFSON, M. M. (1954). *Acta Cryst.* 7, 65–67.

Relations between Integrated Intensities in Crystal Diffraction Methods for X-rays and Neutrons

B. BURAS*
Physical Laboratory II, H. C. Ørsted Institute, University of Copenhagen, DK-2100 Copenhagen, Denmark

AND L. GERWARD
Laboratory of Applied Physics III, Technical University of Denmark, DK-2800 Lyngby, Denmark

In addition to the classical experimental methods of crystal diffraction a number of new methods have become available using the time-of-flight technique for neutrons and energy-dispersive detectors for X-rays. It is shown that there are simple relations between the formulae for the integrated intensities of the different methods, and that the intensity formulae for all the methods can be simply generated, provided that one of them is derived in the usual way. Formulae are given for the powdered crystal and the ideally imperfect crystal in the kinematical approximation as well as for the large perfect crystal in the framework of the dynamical theory.

1. Introduction

The integrated intensity is an important quantity in all diffraction methods used for structure analysis. If a monochromatic beam is used the integration is performed over the scattering angle while in the case of a polychromatic beam the integration is over wavelength. Table 1 summarizes the possible experimental methods and presents the formulae for the integrated intensities in the kinematical approximation. In the

* Also at A.E.C., Risø DK-4000 Roskilde, Denmark.

case of a powdered crystal the formulae apply to the whole Debye–Scherrer ring (cone) and in the case of a rotating single crystal a full (2π) rotation is assumed. We shall refer to the methods in Table 1 as $A1$, $A2$ etc. and discuss them below. The notation used is explained in §§ 2 and 3.

The classical methods are the powder method ($A1$), the Laue method ($B2$) and the monochromatic rotating-crystal method ($A3$). However, in the last few years the time-of-flight (TOF) methods for neutrons and the energy-dispersive spectroscopic (EDS) methods for X-rays have made the remaining methods listed in